

# We are IntechOpen, the world's leading publisher of Open Access books Built by scientists, for scientists

6,900

Open access books available

186,000

International authors and editors

200M

Downloads

Our authors are among the

154

Countries delivered to

TOP 1%

most cited scientists

12.2%

Contributors from top 500 universities



WEB OF SCIENCE™

Selection of our books indexed in the Book Citation Index  
in Web of Science™ Core Collection (BKCI)

Interested in publishing with us?  
Contact [book.department@intechopen.com](mailto:book.department@intechopen.com)

Numbers displayed above are based on latest data collected.  
For more information visit [www.intechopen.com](http://www.intechopen.com)



# Effects of MHD on Modified Nanofluid Model with Variable Viscosity in a Porous Medium

*Sohail Nadeem and Nadeem Abbas*

## Abstract

A computational simulation for two-dimensional steady flow of modified nanofluid over an exponential stretching surface in a porous medium with magnet hydrodynamics and variable viscosity is presented in this study. Modified nanofluids are generalization of both hybrid nanofluids and simple nanofluids. Here, we consider three nanoparticles which drastically enhance the thermal conductivity of nanofluid. The viscous model associated with variable viscosity and MHD flow is employed. Well-known similarity transformations are utilized to convert the partial differential equations to system of ordinary differential equations. These converted equations are solved by utilizing the numerical technique Runge–Kutta-Fehlberg method. The impacts of variable viscosity, porosity parameter, Nusselt number, thermal and velocity slip, skin friction coefficient, solid nanoparticle, and magnetic field are observed. The computational results accomplished in the present investigation are validated and felt to be a good agreement with decayed results. It is highlighted that modified nanofluid model enhances the heat transfer rate much higher than the case of hybrid nanofluid and simple nanofluid model.

**Keywords:** variable viscosity, exponential stretching, modified nanofluid, MHD, porous medium, shooting method

## 1. Introduction

Porous medium is one of the most useful studies due to its applications in the industry and medical sciences. In the medical sciences, it is used in the transport process in the human lungs and kidneys, gall bladder in the presence of stone, clogging in arteries, and also little blood vessels which cannot be opposed. There are several examples of the naturally porous medium such as limestone, wood, seepage of water in river beds, etc. Many researchers are interested to discuss the porous medium due to scientific and technical importance such as earth's science and metallurgy. Such kinds of the flow are analyzed at low Reynolds number in the presence of porous space theoretically. Few researchers were analyzed analytically and experimentally on the porous medium with respect to different aspects (see [1–3]). Recently, the Carreau fluid flow over porous medium in the presence of pressure-dependent viscosity has been discussed by Malik et al. [4]. Some

significant results are analyzed on the porous medium for Newtonian fluids and non-Newtonian fluids with respect to different aspects (see [5–15]) (Figure 1).

In the depth study, flow phenomenon focusing on the variable viscosity and exponentially stretching surface is an important rule in the study of fluid mechanics and has attracted the investigators after its valuable applications in the industry as well as flows detected over the tip of submarine and aircrafts. Numerous methods have been established in recent past years to enhance the fluid thermal conductivity which is suspended with micro-/nano-sized particle mix with base fluid. The nanoparticle possesses chemical and physical properties uniquely because it has been used widely in nanotechnology. The nano-sized particle which is suspended with fluid is called nanofluid. Many investigators investigate about the enhancement of thermal conductivity [16–20] by using the nano-sized particles.

Several experiments have been done in two types of the particles suspended in the base fluid, namely, “hybrid nanofluid.” Basically, such type of fluids is enhances thermal conductivity which was proven through experimental research. Suresh et al. [21, 22] were the first to discuss the idea of hybrid nanofluid through their experimental and numerical results. According to their views, the hybrid nanofluid boosts the heat transfer rate at the surface as compared to nanofluid and simple fluid. These results open a new horizon to the researchers to do a work in the field of hybrid nanofluid. Baghbanzadeh et al. [23] also discussed about the mixture of multiwall/spherical silica nanotube hybrid nanostructures and analysis of thermal conductivity of associated nanofluid. The analysis of  $Al_2O_3$ –MWCNTs with base fluid water and their thermal properties are discussed by Nine et al. [24]. According to them [24], spherical particles with hybrid nanofluid reveal a bit increment in thermal conductivity as related to cylindrical-shaped particle. The hybrid nanofluids are considered experimentally and theoretically by a number of the researchers [25–28].

The physical characteristics of hybrid nanofluid and nanofluid are usually considered constant. It is prominent that the significant physical characteristics of nanofluid and hybrid nanofluid can vary with temperature. For lubricating fluids,

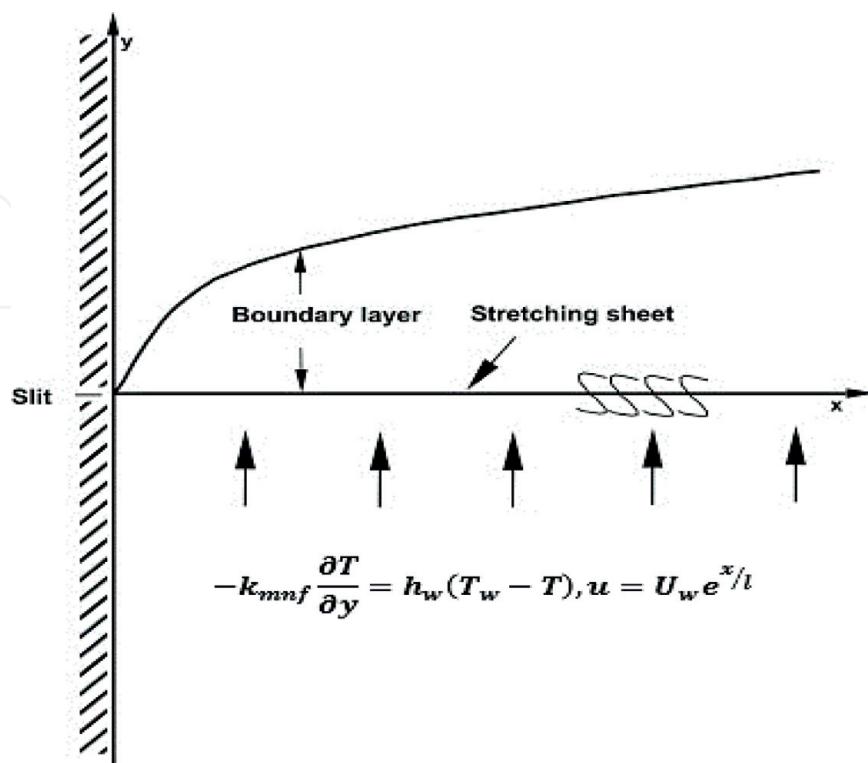


Figure 1.  
Flow pattern of modified nanofluid.

heat generated by the internal friction and the corresponding rise in temperature affects the viscosity of the fluid and so the fluid viscosity can no longer be assumed constant. The increase of temperature leads to a local increase in the transport phenomena by reducing the viscosity across the momentum boundary layer and so the heat transfer rate at the wall is also affected. The impact of thermal radiation and dependent viscosity of fluid on free convective and heat transfer past a porous stretching surface were discussed by Mukhopadhyay and Layek [29]. They gain some significant results for the variable viscosity on the temperature profile and velocity profile. The velocity profile increases and temperature profile decreases for large values of the variable viscosity parameter. The existing literature survey on the variable fluid characteristics and hybrid nanofluid [30–33] reveals that the work is not carried out for hybrid nanofluid over an exponentially stretching surface.

The investigation about the stretching surface has attracted the interest of scientists because of its several applications in the fields of engineering including glass blowing, cooling of microelectronics, quenching in metal foundries, wire drawing, polymer extrusion, rapid spray, etc. Crane [34] discussed about the theoretical boundary layer flow over stretching surface. Various researchers analyzed the exponentially stretching surface [35–38], major applications in the industry and technology.

Here, we study the temperature-dependent viscosity effects on the modified nanofluid flow over an exponentially stretching porous medium in the presence of MHD and Biot number. It is highlighted here that the idea of modified nanofluid has been proposed by us from whom the hybrid nanofluid and simple nanofluid cases can be recovered as a special case. The temperature depends on the Biot number, nanoparticle, and variable viscosity. The system of the flow is illustrated in the form of partial differential equations (PDEs). The system of PDEs is converted into the form of ordinary differential equations (ODEs) by utilizing acceptable similarity transformations. These nonlinear ODEs are solved “numerically” through MATLAB built-in technique. The outcomes are represented through table and graphs.

## 2. Flow formulation

Investigation of steady laminar flow of two-dimensional electrically conducting modified nanofluid over exponentially stretching surface in the presence of variable viscosity has been taken into consideration which is revealed in **Figure 1**.

The fluid flows in the  $x$ -direction and is maintains at a constant wall temperature  $T_w$ . The working fluid is water-based modified nanofluid involving with different types of solid particles ( $Al_2O_3$ ,  $Cu$  and  $Ni$ ) while these particles having nanosized. These three particles are suspended with base fluid water. Some assumptions of these solid particles are following in this study like as negligible internal heat generation, incompressible flow, negligible radiative heat transfer and no chemical reaction. The thermophysical characteristics of modified nanofluid are represented in **Table 1**.

Under these assumptions with the usual boundary layer approximation, the governing differential equations of mass, momentum, and energy for the problem under consideration are defined as follows:

$$\frac{\partial u}{\partial x} + \frac{\partial v}{\partial y} = 0, \quad (1)$$

$$u \frac{\partial u}{\partial x} + v \frac{\partial u}{\partial y} = \frac{1}{\rho_{mnf}} \frac{\partial}{\partial y} \left( \mu_{mnf} \frac{\partial u}{\partial y} \right) - \frac{\sigma B_0^2}{\rho_{mnf}} u - \frac{\nu_{mnf}}{R} u, \quad (2)$$

Thermophysical properties	Fluidphase (water)	Al <sub>2</sub> O <sub>3</sub>	Cu	Ni
C <sub>p</sub> (j/kg)K	4179	765	385	444
ρ(kg/m <sup>3</sup> )	997.1	3970	8933	8900
k(W/mK)	0.613	40	400	90.7

**Table 1.**  
Numerical values of nanoparticles and water.

$$u \frac{\partial T}{\partial x} + v \frac{\partial T}{\partial y} = \alpha_{mnf} \frac{\partial^2 T}{\partial y^2}, \quad (3)$$

The appropriated boundary conditions are stated as

$$u \rightarrow U_w, \quad -k_{mnf} \frac{\partial T}{\partial y} = h(T_w - T), \quad \text{as } y \rightarrow 0, \quad (4)$$

$$u \rightarrow 0, \quad T \rightarrow T_\infty, \quad \text{as } y \rightarrow \infty,$$

where  $u$  and  $v$  are the fluid velocity components in the  $x$  and  $y$  directions, respectively,  $T$  is the fluid temperature,  $U_0$  is denoted as the stream velocity, and  $T_\infty$  represents as the temperature of the fluid far away from the surface. The thermophysical properties of nanofluid, hybrid nanofluid, and modified nanofluid are represented in **Tables 2** and **3**.

An extraordinary type of physical characteristics is acquainted in the present examination to investigate the boundary layer equations for modified nanofluid. Modified nanofluid is deliberated through taking the combination of Al<sub>2</sub>O<sub>3</sub> and Cu with base fluid water. The nanoparticles Al<sub>2</sub>O<sub>3</sub> and Cu ( $\Phi_1 = 0.05 \text{ vol}$  and  $\Phi_2 = 0.05 \text{ vol}$ , respectively) are fixed throughout this problem. To make it ideal, the final type of the powerful thermophysical characteristics of (Al<sub>2</sub>O<sub>3</sub>/water) nanofluid, (Al<sub>2</sub>O<sub>3</sub> – Cu/water) hybrid nanofluid and (Al<sub>2</sub>O<sub>3</sub> – Cu – Ni/water) modified nanofluid, is assumed in **Tables 2** and **3**, while  $n = 3$  is for spherical nanoparticles. Some subscripts are defined as following, solid nanoparticles of Al<sub>2</sub>O<sub>3</sub>,  $s_2$  solid nanoparticles of the Cu,  $s_3$  solid nanoparticles of Ni,  $f$  for base fluid (water),  $nf$  for nanofluid,  $hnf$  for Hybrid nanofluid and  $mnf$  for modified nanofluid. The thermophysical characteristics of fluid are represented in **Table 1** at 25° C where  $U_w = U_0 e^{\frac{x}{L}}$ ,  $T_w = T_\infty + T_0 e^{\frac{x}{L}}$ . The  $\mu_f$  is the coefficient of the viscosity which is assumed to vary as an inverse function of temperature [23] as

Properties	Nanofluid	Hybrid nano-fluid
Density	$\rho_{nf} = (1 - \Phi)\rho_f + \Phi\rho_s$	$\rho_{hnf} = \{[(1 - \Phi_2)(1 - \Phi_1)\rho_f] + \Phi_1\rho_{s_1}\} + \Phi_2\rho_{s_2}$
Heat capacity	$(\rho C_p)_{nf} = (1 - \Phi)(\rho C_p)_f + \Phi(\rho C_p)_s$	$(\rho C_p)_{hnf} = \{[(1 - \Phi_2)(1 - \Phi_1)(\rho C_p)_f] + \Phi_1(\rho C_p)_{s_1}\} + \Phi_2\rho(\rho C_p)_{s_2}$
Viscosity	$\mu_{nf} = \frac{\mu_f}{(1 - \Phi)^{2.5}}$	$\mu_{hnf} = \frac{\mu_f}{(1 - \Phi_1)^{2.5}(1 - \Phi_2)^{2.5}}$
Thermal conductivity	$\frac{\kappa_{nf}}{\kappa_f} = \frac{\kappa_s + (n - 1)\kappa_f - (n - 1)\Phi(\kappa_f - \kappa_s)}{\kappa_s + (n - 1)\kappa_f + \Phi(\kappa_f - \kappa_s)}$	$\frac{\kappa_{hnf}}{\kappa_{bf}} = \frac{\kappa_{s_2} + (n - 1)\kappa_{bf} - (n - 1)\Phi_2(\kappa_{bf} - \kappa_{s_2})}{\kappa_{s_2} + (n - 1)\kappa_{bf} + \Phi_2(\kappa_{bf} - \kappa_{s_2})}$ where $\frac{\kappa_{bf}}{\kappa_f} = \frac{\kappa_{s_1} + (n - 1)\kappa_f - (n - 1)\Phi_1(\kappa_f - \kappa_{s_1})}{\kappa_{s_1} + (n - 1)\kappa_f + \Phi_1(\kappa_f - \kappa_{s_1})}$

**Table 2.**  
Physical Properties of Nanofluid and Hybrid Nanofluid.

Properties	Modified nanofluid
Density	$\rho_{mnf} = (1 - \Phi_3) \left( \left[ \{ (1 - \Phi_2)(1 - \Phi_1)\rho_f \} + \Phi_1\rho_{s_1} \right] + \Phi_2\rho_{s_2} \right) + \Phi_3\rho_{s_3}$
Heat capacity	$(\rho C_p)_{mnf} = (1 - \Phi_3) \left( \left[ \{ (1 - \Phi_2)(1 - \Phi_1)(\rho C_p)_f \} + \Phi_1(\rho C_p)_{s_1} \right] + \Phi_2(\rho C_p)_{s_2} \right) + \Phi_3(\rho C_p)_{s_3}$
Viscosity	$\mu_{mnf} = \frac{\mu_f}{(1 - \Phi_3)^{2.5}(1 - \Phi_1)^{2.5}(1 - \Phi_2)^{2.5}}$
Thermal conductivity	$\frac{\kappa_{nf}}{\kappa_f} = \frac{\kappa_{s_1} + (n - 1)\kappa_f - (n - 1)\Phi_1(\kappa_f - \kappa_{s_1})}{\kappa_{s_1} + (n - 1)\kappa_f + \Phi_1(\kappa_f - \kappa_{s_1})}$ $\frac{\kappa_{hnf}}{\kappa_{nf}} = \frac{\kappa_{s_2} + (n - 1)\kappa_{nf} - (n - 1)\Phi_2(\kappa_{nf} - \kappa_{s_2})}{\kappa_{s_2} + (n - 1)\kappa_{nf} + \Phi_2(\kappa_{nf} - \kappa_{s_2})}$ $\frac{\kappa_{mnf}}{\kappa_{hnf}} = \frac{\kappa_{s_3} + (n - 1)\kappa_{hnf} - (n - 1)\Phi_3(\kappa_{hnf} - \kappa_{s_3})}{\kappa_{s_3} + (n - 1)\kappa_{hnf} + \Phi_3(\kappa_{hnf} - \kappa_{s_3})}$

**Table 3.**  
 Physical Properties Modified Nanofluid.

$$\frac{1}{\mu} = \frac{1}{\mu_f} [1 + \delta(T - T_r)], \quad (5)$$

i.e.,  $\frac{1}{\mu_f} = a(T - T_\infty)$  where  $a = \frac{\delta}{\mu_f}$  and  $T_r = T_\infty - \frac{1}{\delta}$ .

$$u = U_0 e^{x/l} f'(\zeta), \quad v = -\frac{\nu}{l} \sqrt{\frac{Re}{2}} e^{x/2l} (f(\zeta) + \zeta f'(\zeta)), \quad (6)$$

$$T = T_\infty + T_w e^{x/2l} \theta(\zeta), \quad \zeta = \frac{y}{l} \sqrt{\frac{Re}{2}} e^{x/2l}, \quad (7)$$

The mathematical model over exponentially stretching surface is chosen to allow the coupled non-linear partial differential equations are converted into coupled non-linear ordinary differential equations by using the suitable similarity transformation which is given above. Where  $\zeta$  is the similarity variable and  $\theta$  and  $f$  are the dimensionless temperature and velocity, respectively. Eq. (1) is directly satisfied by using the similarities which is called continuity equation. The momentum and energy equation are written as

$$\frac{\left( \frac{f'''}{1 - \frac{\theta}{\theta_e}} + \frac{f''\theta'}{\theta_e \left(1 - \frac{\theta}{\theta_e}\right)^2} \right)}{(1 - \Phi_3)^{2.5}(1 - \Phi_2)^{2.5}(1 - \Phi_1)^{2.5} \left[ (1 - \Phi_3) \left\{ (1 - \Phi_2) \left( 1 - \Phi_1 + \Phi_1 \frac{\rho_{s_1}}{\rho_f} \right) + \Phi_2 \frac{\rho_{s_2}}{\rho_f} \right\} + \Phi_3 \frac{\rho_{s_3}}{\rho_f} \right]} - \beta f' f' + f f'' - M^2 f' - \beta f' = 0, \quad \beta = 2; \quad (8)$$

$$\frac{\frac{\kappa_{mnf}}{\kappa_f} \theta''}{Pr \left[ (1 - \Phi_3) \left( \left\{ (1 - \Phi_2) \left( 1 - \Phi_1 + \Phi_1 \frac{(\rho C_p)_{s_1}}{(\rho C_p)_f} \right) \right\} + \Phi_2 \frac{(\rho C_p)_{s_2}}{(\rho C_p)_f} \right) + \Phi_3 \frac{(\rho C_p)_{s_3}}{(\rho C_p)_f} \right]} - \theta f' + \theta' f = 0 \quad (9)$$

with boundary conditions

$$f'(0) = 1, \quad f(0) = 0, \quad f'(\infty) = 0 \quad (10)$$

$$\theta'(0) = -\gamma \left( \frac{k_f}{k_{mnf}} \right) (1 - \theta(0)), \quad \theta(\infty) = 0 \quad (11)$$

### 3. Numerical solution method

Boundary layer heat transfer and modified nanofluid flow of an exponentially stretching surface with ( $Al_2O_3 - Cu - Ni$ ) under the assumption of dependent fluid viscosity, magnetic field, and thermal slip effects are computed here. The results of boundary layer problem are obtained numerically through `bvp4c` method. The notable highlights of the flow and heat transfer characteristics are achieved utilizing the modified nanofluid. Keeping in mind the end goal to get clear knowledge of the physical problem, the results are given through the physical parameter, namely, magnetic field ( $M$ ), solid nanoparticle ( $\Phi_3$ ) and thermal slip effects ( $Bi$ ) and ( $\theta_e$ ). The numerical results are represented in the form of tables.

$$y(1) = f(\zeta),$$

$$y(2) = f'(\zeta),$$

$$y(3) = f''(\zeta),$$

$$f''(\zeta) = \left( 1 - \frac{y(4)}{\theta_e} \right) \left\{ -\frac{y(3)y(5)}{\theta_e \left( 1 - \frac{y(4)}{\theta_e} \right)^2} + (1 - \Phi_3)^{2.5} (1 - \Phi_2)^{2.5} (1 - \Phi_1)^{2.5} \left[ (1 - \Phi_3) \left\{ (1 - \Phi_2) \left( 1 - \Phi_1 + \Phi_1 \frac{\rho_{s1}}{\rho_f} \right) + \Phi_2 \frac{\rho_{s2}}{\rho_f} \right\} + \Phi_3 \frac{\rho_{s3}}{\rho_f} \right] + 2y(2)y(2) - y(1)y(3) + M^2 y(2) \right\},$$

$$y(4) = \theta(\zeta),$$

$$y(5) = \theta'(\zeta),$$

$$\theta'' = \frac{\kappa_f \text{Pr} \left[ (1 - \Phi_3) \left( \left\{ (1 - \Phi_2) \left( 1 - \Phi_1 + \Phi_1 \frac{(\rho C_p)_{s1}}{(\rho C_p)_f} \right) \right\} + \Phi_2 \frac{(\rho C_p)_{s2}}{(\rho C_p)_f} \right) + \Phi_3 \frac{(\rho C_p)_{s3}}{(\rho C_p)_f} \right]}{\kappa_{mnf}} (y(5)y(1) - y(4)y(2)),$$

subject to the boundary conditions

$$y(2) = 1, \quad y(1) = 0, \quad yinf(2) = 0,$$

$$y(5) = -\gamma \left( \frac{k_f}{k_{mnf}} \right) (1 - y(4)), \quad yinf(4) = 0.$$

For brevity, the points of interest of the solution strategy are not performed here. The heat transfer and modified nanofluid are effected by dependent viscosity parameter and MHD; the fundamental focus of our investigation is to bring out the impacts of these parameters by the numerical solution. It is worth specifying that we have utilized the information displayed in **Tables 1–3** for the thermophysical properties of the fluid, nanofluid, hybrid nanofluid, modified nanofluid, and nanoparticles. Three types of the nanoparticles are used, namely,  $Al_2O_3$ ,  $Cu$ , and  $Ni$ . The Nussle number

and skin friction coefficient are the most important features of this study. For practical purposes, the functions  $\theta(\zeta)$  and  $f(\zeta)$  allow to determine the Nusselt number:

$$Nu_x = -\frac{xk_{mnf}}{k_f(T_w - T_\infty)} \left( \frac{\partial T(x, y)}{\partial y} \right)_{y=0}, \quad (12)$$

$$\frac{Nu_x}{\sqrt{Re_x}} = -\frac{k_f}{k_{mnf}} \theta'(0) \quad (13)$$

and skin friction coefficient

$$C_f = \frac{\mu_{mnf}}{\rho_f u_w^2} \left( \frac{\partial u(x, y)}{\partial y} \right)_{y=0}, \quad (14)$$

$$\frac{C_f}{\sqrt{Re_x}} = -\frac{1}{(1 - \varphi_3)^{2.5}(1 - \varphi_2)^{2.5}(1 - \varphi_1)^{2.5}} \left( 1 - \frac{1}{\theta_e} \right)^{-1} f''(0). \quad (15)$$

Here, the local Reynolds number is  $Re_x = \frac{xu_w}{\nu_f}$ .

#### 4. Numerical results

The impact of dependent viscosity parameter  $\theta_e$  on the coefficient of skin friction and Nusselt number for negative values of  $\theta_e$  (for liquids) and for positive values of  $\theta_e$  (for gases) which reveals in **Table 4**. The variation of  $f''(0)$  and  $\theta'(0)$  reveals that the same behavior to be noted for large values of  $\theta_e$ .

The computational results are shown in **Table 5**. The velocity of the flow decreases due to increase in the solid nanoparticle of  $Ni$  ( $\Phi_3$ ), as well as skin fraction is decreased. This may be due to more collision between the suspended nanoparticles. The nanoparticles release the energy in the form of heat by physically. Adding more particles may exert more energy which increases the temperature while also thickness of the thermal boundary layer. The increment of solid nanoparticle accelerates the flow velocity which obviously declines the skin fraction which is shown in **Table 5**. It is also seen that  $\theta'(0)$  decreases due to increasing the solid nanoparticles ( $Ni$  ( $\Phi_3$ )). It is noted in **Table 5** that the magnetic field parameter increases due to decrease in the velocity flow of the modified nanofluid. For the large values of the magnetic field, the dimensionless rate of heat transfer gains

$\theta_e$	$Al_2O_3 - Cu - Ni/water$		$Al_2O_3 - Ni/water$	
	$f''(0)$	$\theta'(0)$	$f''(0)$	$\theta'(0)$
-10	-1.98532	-1.7779	-1.90976	-1.98809
-5	-2.07138	-1.77154	-1.99315	-1.98175
-1	-2.65068	-1.72622	-2.55803	-1.93639
-0.1	-5.21601	-1.49115	-5.08404	-1.69636
1	-0.768213	-1.85951	-0.731972	-2.06964
5	-1.70487	-1.79801	-1.63866	-2.00813
10	-1.80225	-1.79113	-1.7327	-2.00127

**Table 4.** Computational results of  $Al_2O_3 - Cu - Ni/water$  and  $Al_2O_3 - Ni/water$ .

$\gamma$	$Bi$	$M$	$\Phi_3$	$Al_2O_3-Cu-Ni/water$		$Al_2O_3-Ni/water$	
				$f''(0)$	$\theta'(0)$	$f''(0)$	$\theta'(0)$
0.0				-1.50718	-1.86066	-1.44127	-2.07585
0.5				-1.6881	-1.83996	-1.61326	-2.05562
1.0				-1.8533	-1.82077	-1.77026	-2.03689
0.5	0.0			-1.58519	-2.79411	-1.52063	-3.06462
	0.2			-1.6881	-1.83996	-1.61326	-2.05562
	0.4			-1.73712	-1.37364	-1.65867	-1.54835
	0.2	0.0		-1.50718	-1.86066	-1.44127	-2.07585
		0.5		-1.6881	-1.83996	-1.61326	-2.05562
		1.0		-1.8533	-1.82077	-1.77026	-2.03689
		0.5	0.005	-1.6158	-1.99761	-1.5041	-2.23451
			0.04	-1.6881	-1.83996	-1.61326	-2.05562
			0.08	-1.74614	-1.67941	-1.70227	-1.87409

**Table 5.** Computational results of  $Al_2O_3 - Cu - Ni/water$  and  $Al_2O_3 - Ni/water$  fixed at  $\theta_e=0.5$ .

enhanced in the Modified nanofluid. A dimensionless quantity is the Biot number which compares the relative transport of internal and external resistances. The dimensionless  $f''(0)$  and  $\theta'(0)$  increase for large values of the Biot numbers. The dimensionless of  $\theta'(0)$  gets decreases for the increment of Biot number while the dimensionless of  $f''(0)$  gets increases for the increment of Biot number as shown in **Table 5** for the modified nanofluid. The Biot number is directly

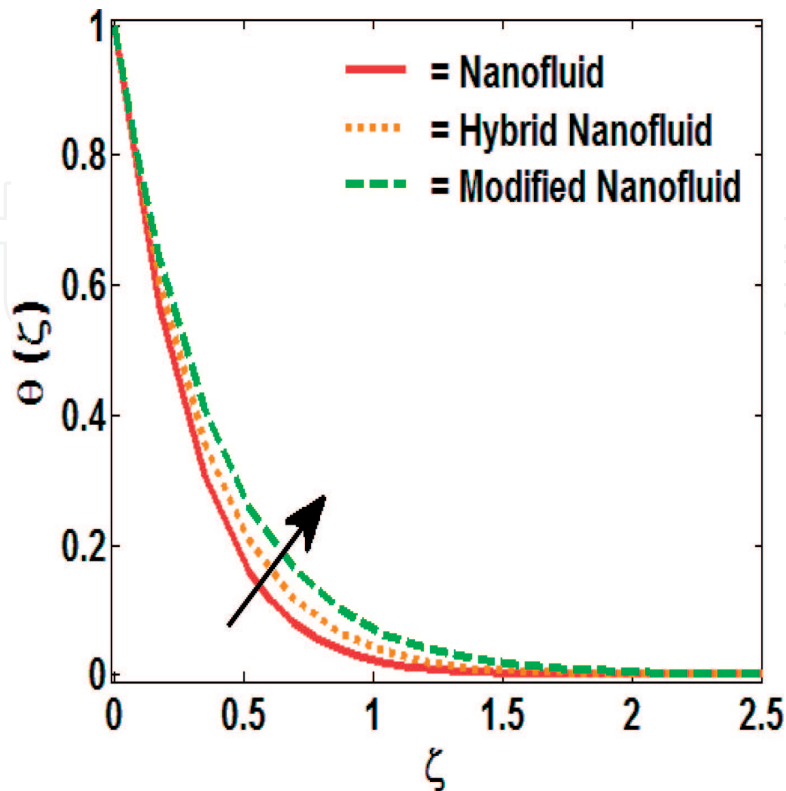


**Figure 2.** Comparative results of Nanofluid, Hybrid nanofluid and Modified nanofluid on  $\theta(\zeta)$ .

proportional to the heat transfer coefficient. It is also seen that the variable viscosity parameter declines for enhancing the dimensionless  $f''(0)$  of the modified nanofluid. It is also noted that the heat transfer rate declines due to increase in the variable viscosity parameter as shown in **Table 5**. Effects of porosity parameter on the  $f''(0)$  and  $\theta'(0)$  are presented in **Table 5**. It is highlighted that  $f''(0)$  increased for the higher values of the porosity parameter but had an opposite behavior to be highlighted for  $\theta'(0)$ . **Figure 2** shows the impacts of comparative study of modified nanofluid, hybrid nanofluid and simple nanofluid.

## 5. Graphical results

The temperature profile shows the variation of solid nanoparticle in **Figure 3**. The nanoparticle dissipates energy in the form of heat. So, the mixture of more nanoparticles may exert more energy which increases the thickness of the boundary layer and temperature.

**Figure 4** reveals the impacts of solid particle on velocity profiles. The velocity profile gets decelerated due to increase in solid nanoparticle for modified nanofluid. This phenomenon exists due to more collision with suspended nanoparticles.

**Figure 5** reveals the effects of magnetic field on the velocity profile. Being there, the transverse magnetic field creates Lorentz force which arises from the attraction of electric field and magnetic field during the motion of an electrically conducting fluid. The velocity profile decreases for the positive values of magnetic field parameter. Because the resisting force increases and consequently velocity declines in the  $x$ -direction with boundary layer thickness as the magnetic field parameter enhances for modified nanofluid.

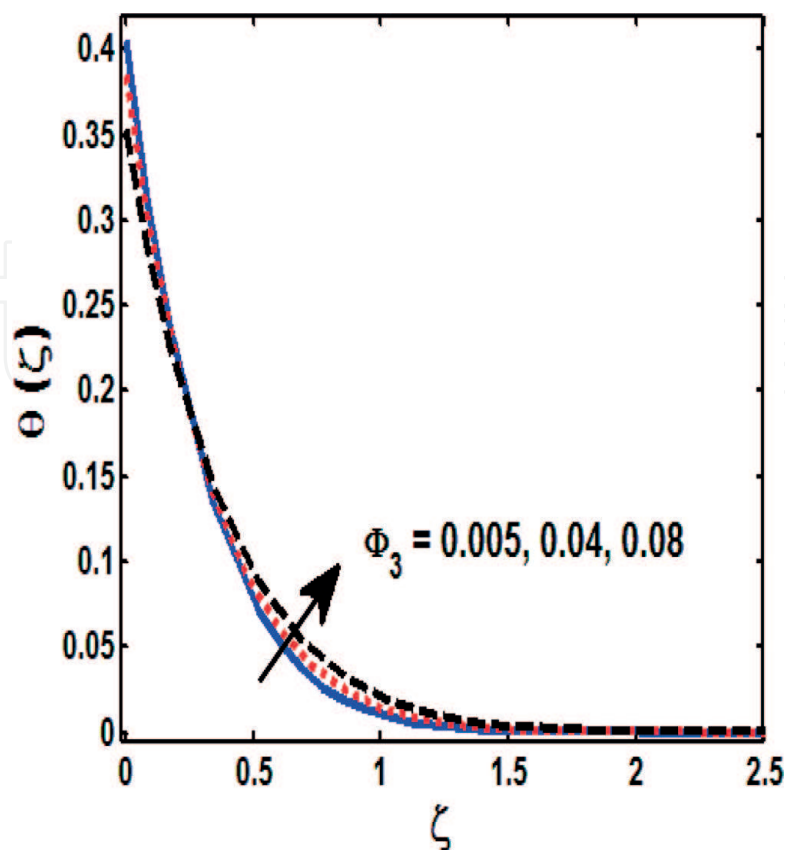


**Figure 3.**  
Impacts of  $\Phi_3$  on temperature profile.

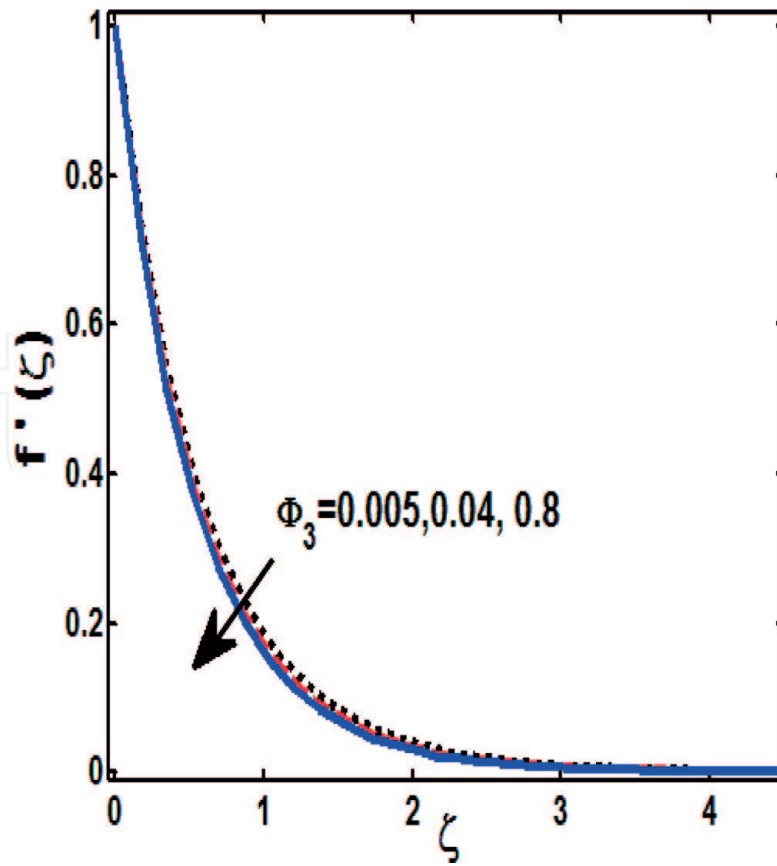


Figure 4.  
Impacts of  $\Phi_3$  on velocity profile.

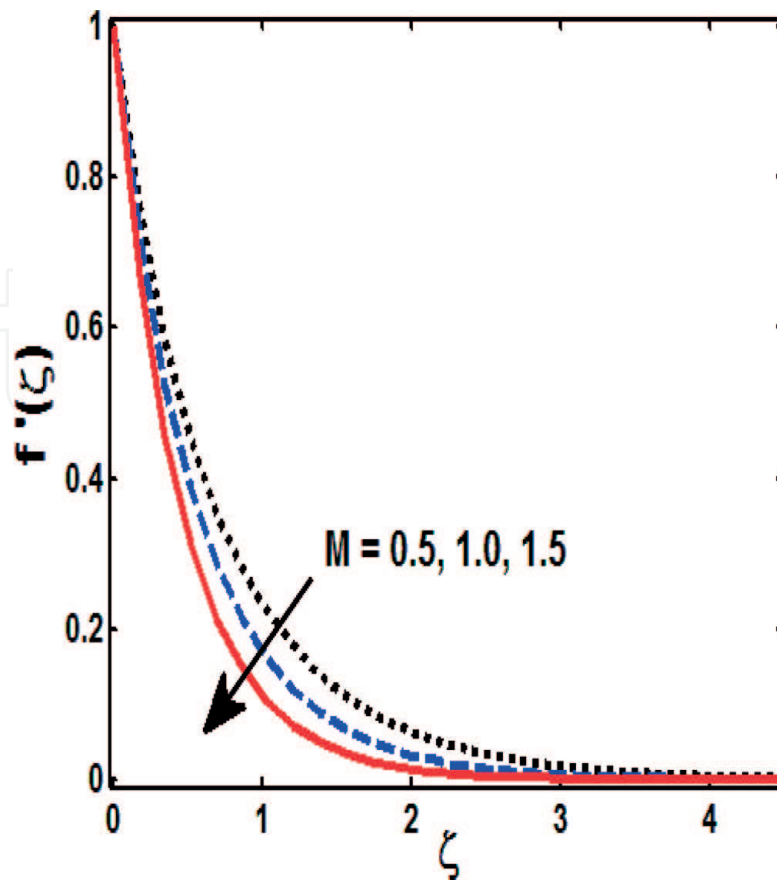


Figure 5.  
Impacts of  $M$  on the velocity profile.

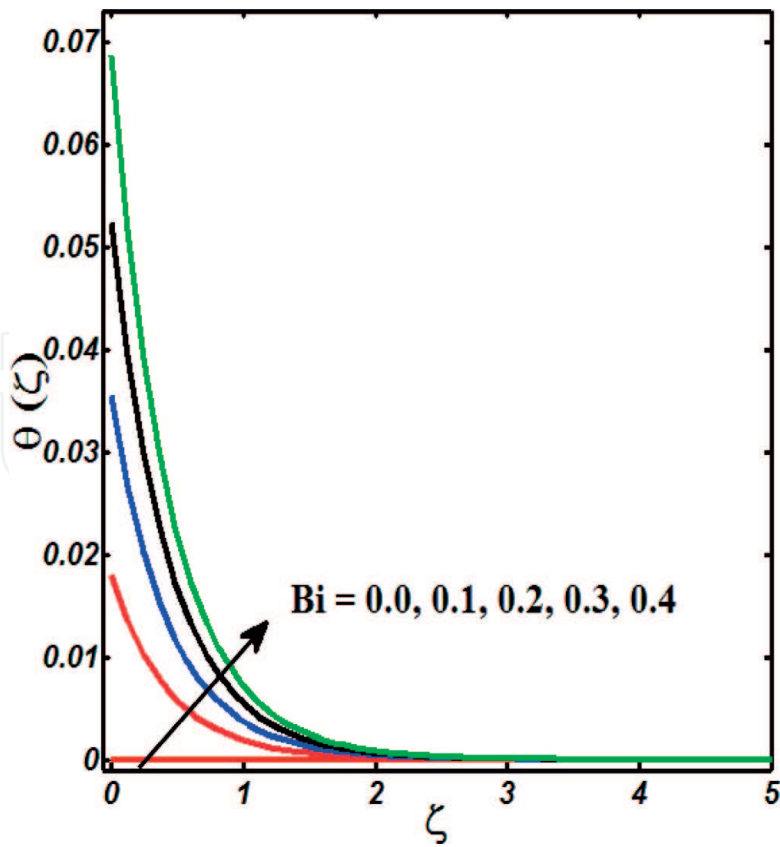


Figure 6.  
Impacts of  $Bi$  on the temperature profile.

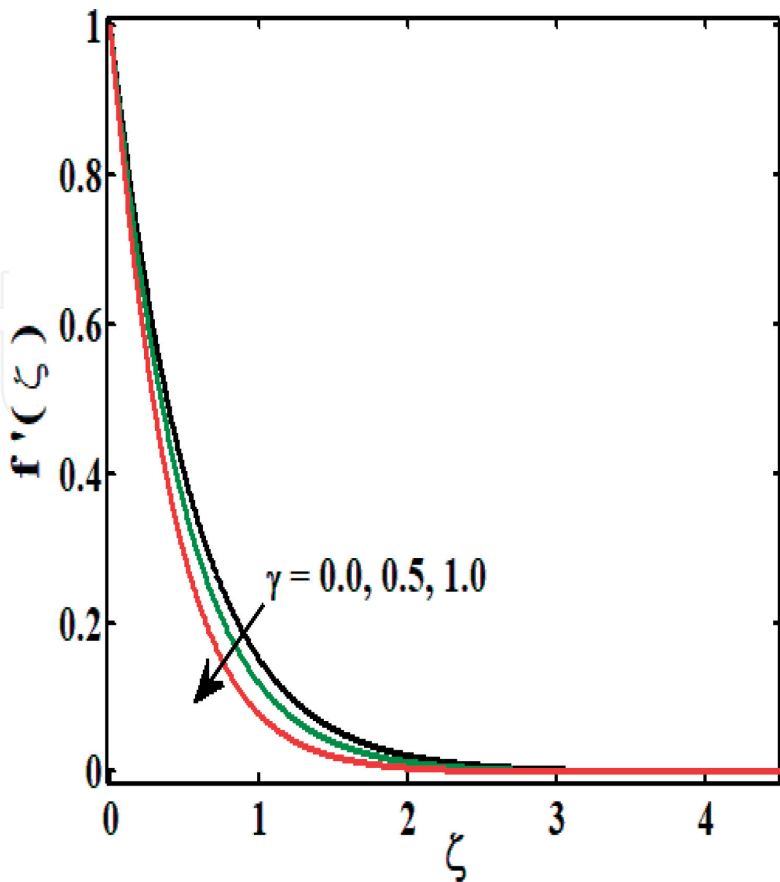


Figure 7.  
Impacts of  $\gamma$  on velocity profile.

**Figure 6** reveals the variation of dimensionless quantity of Biot number on the temperature profile. The relative transport of internal and external resistances is called the Biot number. The thermal boundary layer increases with increasing in the biot number.

**Figure 7** shows the impact of the porosity parameter on the velocity profile. It is noted that velocity profiles decreases for the higher values of the porosity parameter. The boundary layer thickness decreases for large values of porosity parameter.

## 6. Closing remarks

In this paper, the impacts of dependent viscosity parameter, magnetic field, and solid nanoparticle flow and the heat transfer of modified nanofluid flow at the exponential stretching surface have been analyzed numerically. The governing coupled partial differential equations are converted into ordinary coupled differential equations which are solved numerically by bvp4c method. The parametric analysis is executed to investigate the impacts of the governing physical parameters (magnetic field, variable viscosity (for both cases  $\theta_e < 0$  and  $\theta_e > 0$ ), Biot number, and solid nanoparticle) on the flow and heat transfer properties. In particular, we focus on the effect of dependent viscosity when  $\theta_e < 0$  and  $\theta_e > 0$  of the  $Al_2O_3 - Cu - Ni/water$  and  $Al_2O_3 - Ni/water$ . It is noted that the fluid viscosity and temperature are inverse function. The computational results are presented through graph and tables. The results of modified nanofluid flow and heat transfer properties show many exciting behaviors which deserve further study of modified nanofluid.

## Nomenclature

Pr	Prandtl number
$\Phi_1$	nanoparticle volume fraction of $Al_2O_3$
$\Phi_2$	nanoparticle volume fraction of Cu
$\Phi_3$	nanoparticle volume fraction of Ni
$Bi$	Biot number
$\theta$	temperature profile
$R$	permeability
$f$	velocity profile along x-direction
$\rho$	density
$f$	fluid
$T_w$	wall temperature
$T_\infty$	ambient temperature
$\nu_f$	fluid kinematic viscosity
$\nu_{nf}$	nanofluid kinematic viscosity
$\nu_{hmf}$	hybrid nanofluid kinematic viscosity
$\nu_{mnf}$	modified nanofluid kinematic viscosity
$(\rho C_p)_{hmf}$	heat capacity of hybrid nanofluid
$(\rho C_p)_{mnf}$	heat capacity of modified nanofluid
$\kappa_f$	thermal conductivity of fluid
$\kappa_{nf}$	thermal conductivity of nanofluid
$\kappa_{hmf}$	thermal conductivity of hybrid nanofluid

$\kappa_{mnf}$	thermal conductivity of modified nanofluid
$\mu_{hnf}$	viscosity of hybrid nanofluid
$\mu_{mnf}$	viscosity of modified nanofluid
$\mu_{nf}$	viscosity of nanofluid
$(\rho C_p)_{nf}$	heat capacity of nanofluid
$\alpha_{hnf}$	thermal diffusivity of hybrid nanofluid
$\alpha_{mnf}$	thermal diffusivity of modified nanofluid
$\alpha_{nf}$	thermal diffusivity of nanofluid
$U, V$	velocity components
$X, Y$	direction components
$\theta_e$	variable viscosity parameter
$\gamma$	porosity parameter

IntechOpen

## Author details

Sohail Nadeem and Nadeem Abbas\*

Department of Mathematics, Quaid-I-Azam University, Islamabad, Pakistan

\*Address all correspondence to: [nabbas@math.qau.edu.pk](mailto:nabbas@math.qau.edu.pk)

## IntechOpen

© 2019 The Author(s). Licensee IntechOpen. This chapter is distributed under the terms of the Creative Commons Attribution License (<http://creativecommons.org/licenses/by/3.0/>), which permits unrestricted use, distribution, and reproduction in any medium, provided the original work is properly cited. 

## References

- [1] Ping C, Chang ID. Buoyancy induced flows in a saturated porous medium adjacent to impermeable horizontal surfaces. *International Journal of Heat and Mass Transfer*. 1976;**19**(11): 1267-1272
- [2] Caltagirone JP. Thermoconvective instabilities in a porous medium bounded by two concentric horizontal cylinders. *Journal of Fluid Mechanics*. 1976;**76**(2):337-362
- [3] Yamamoto K, Iwamura N. Flow with convective acceleration through a porous medium. *Journal of Engineering Mathematics*. 1976;**10**(1):41-54
- [4] Malik MY, Zehra I, Nadeem S. Flows of Carreau fluid with pressure dependent viscosity in a variable porous medium: Application of polymer melt. *Alexandria Engineering Journal*. 2014; **53**(2):427-435
- [5] Subhani M, Nadeem S. Numerical analysis of 3D micropolar nanofluid flow induced by an exponentially stretching surface embedded in a porous medium. *The European Physical Journal Plus*. 2017;**132**(10):441
- [6] Sheikholeslami M, Jafaryar M, Saleem S, Li Z, Shafee A, Jiang Y. Nanofluid heat transfer augmentation and exergy loss inside a pipe equipped with innovative turbulators. *International Journal of Heat and Mass Transfer*. 2018;**126**:156-163
- [7] Sheikholeslami M. Finite element method for PCM solidification in existence of CuO nanoparticles. *Journal of Molecular Liquids*. 2018;**265**:347-355
- [8] Sheikholeslami M, Li Z, Shafee A. Lorentz forces effect on NEPCM heat transfer during solidification in a porous energy storage system. *International Journal of Heat and Mass Transfer*. 2018;**127**:665-674
- [9] Sheikholeslami M. Application of Darcy law for nanofluid flow in a porous cavity under the impact of Lorentz forces. *Journal of Molecular Liquids*. 2018;**266**:495-503
- [10] Ahmad S, Farooq M, Anjum A, Javed M, Malik MY, Alshomrani AS. Diffusive species in MHD squeezed fluid flow through non-Darcy porous medium with viscous dissipation and joule heating. *Journal of Magnetism*. 2018;**23**(2):323-332
- [11] Sheikholeslami M, Shehzad SA, Li Z, Shafee A. Numerical modeling for alumina nanofluid magnetohydrodynamic convective heat transfer in a permeable medium using Darcy law. *International Journal of Heat and Mass Transfer*. 2018;**127**:614-622
- [12] Sheikholeslami M, Jafaryar M, Li Z. Second law analysis for nanofluid turbulent flow inside a circular duct in presence of twisted tape turbulators. *Journal of Molecular Liquids*. 2018;**263**: 489-500
- [13] Sheikholeslami M. Influence of magnetic field on  $Al_2O_3$ - $H_2O$  nanofluid forced convection heat transfer in a porous lid driven cavity with hot sphere obstacle by means of LBM. *Journal of Molecular Liquids*. 2018;**263**: 472-488
- [14] Sheikholeslami M. Numerical approach for MHD  $Al_2O_3$ -water nanofluid transportation inside a permeable medium using innovative computer method. *Computer Methods in Applied Mechanics and Engineering*. 2019;**344**:306-318
- [15] Sheikholeslami M. New computational approach for exergy and entropy analysis of nanofluid under the impact of Lorentz force through a porous media. *Computer Methods in*

Applied Mechanics and Engineering.  
2019;**344**:319-333

[16] Choi S, Zhang ZG, Yu W, et al. Anomalously thermal conductivity enhancement in nanotube suspensions. *Applied Physics Letters*. 2001;**79**(14): 2252-2254

[17] Khan I, Fatima S, Malik MY, Salahuddin T. Exponentially Varying Viscosity of Magneto hydrodynamic Mixed Convection Eyring-Powell Nanofluid Flow Over An Inclined Surface. *Results in Physics*; 2018;**8**: 1194-1203

[18] Nadeem S, Abbas N. On Both MHD and Slip Effect in Micropolar Hybrid Nanofluid Past a Circular Cylinder Under Stagnation Point Region. *Canadian Journal of Physics*, (ja)

[19] Sadaf H, Akbar MU, Nadeem S. Induced magnetic field analysis for the peristaltic transport of non-Newtonian nanofluid in an annulus. *Mathematics and Computers in Simulation*. 2018;**148**: 16-36

[20] Sheikholeslami M, Gerdroodbary MB, Moradi R, Shafee A, Li Z. Application of Neural Network for estimation of heat transfer treatment of  $\text{Al}_2\text{O}_3\text{-H}_2\text{O}$  nanofluid through a channel. *Computer Methods in Applied Mechanics and Engineering*. 2019;**344**: 1-12

[21] Suresh S, Venkitaraj KP, Selvakumar P, Chandrasekar M. Synthesis of  $\text{Al}_2\text{O}_3\text{-Cu}$ /water hybrid nanofluids using two step method and its thermo physical properties. *Colloids and Surfaces A: Physicochemical and Engineering Aspects*. 2011;**388**(1-3): 41-48

[22] Suresh S, Venkitaraj KP, Selvakumar P, Chandrasekar M. Effect of  $\text{Al}_2\text{O}_3\text{-Cu}$ /water hybrid nanofluid in heat transfer. *Experimental Thermal and Fluid Science*. 2012;**38**:54-60

[23] Baghbanzadeh M, Rashidi A, Rashtchian D, Lotfi R, Amrollahi A. Synthesis of spherical silica/multiwall carbon nanotubes hybrid nanostructures and investigation of thermal conductivity of related nanofluids. *Thermochimica Acta*. 2012; **549**:87-94

[24] Esfe MH, Arani AAA, Rezaie M, Yan WM, Karimipour A. Experimental determination of thermal conductivity and dynamic viscosity of  $\text{Ag-MgO}$ /water hybrid nanofluid. *International Communications in Heat and Mass Transfer*. 2015;**66**:189-195

[25] Hayat T, Nadeem S. Heat transfer enhancement with  $\text{Ag-CuO}$ /water hybrid nanofluid. *Results in Physics*. 2017;**7**:2317-2324

[26] Muhammad N, Nadeem S. Ferrite nanoparticles  $\text{Ni-ZnFe}_2\text{O}_4$ ,  $\text{Mn-ZnFe}_2\text{O}_4$  and  $\text{Fe}_2\text{O}_4$  in the flow of ferromagnetic nanofluid. *The European Physical Journal Plus*. 2017;**132**(9):377

[27] Ijaz S, Nadeem S. Biomedical theoretical investigation of blood mediated nanoparticles ( $\text{Ag-Al}_2\text{O}_3$ /blood) impact on hemodynamics of overlapped stenotic artery. *Journal of Molecular Liquids*. 2017;**248**:809-821

[28] Nadeem S, Abbas N, Khan AU. Characteristics of Three Dimensional Stagnation Point Flow of Hybrid Nanofluid Past A Circular Cylinder. *Results in Physics*; 2018

[29] Mukhopadhyay S, Layek GC. Effects of thermal radiation and variable fluid viscosity on free convective flow and heat transfer past a porous stretching surface. *International Journal of Heat and Mass Transfer*. 2008; **51**(9-10):2167-2178

[30] Vajravelu K, Prasad KV, Chiu-On NG. The effect of variable viscosity on the flow and heat transfer of a viscous

Ag-water and Cu-water nanofluids. *Journal of Hydrodynamics, Ser. B.* 2013; **25**(1):1-9

[31] Sheikholeslami M, Gorji-Bandpy M, Vajravelu K. Lattice Boltzmann simulation of magnetohydrodynamic natural convection heat transfer of  $\text{Al}_2\text{O}_3$ -water nanofluid in a horizontal cylindrical enclosure with an inner triangular cylinder. *International Journal of Heat and Mass Transfer.* 2015; **80**:16-25

[32] Khan WA, Makinde OD, Khan ZH. Non-aligned MHD stagnation point flow of variable viscosity nanofluids past a stretching sheet with radiative heat. *International Journal of Heat and Mass Transfer.* 2016; **96**:525-534

[33] Konch J, Hazarika G. Effects of variable viscosity and variable thermal conductivity on hydromagnetic dusty fluid flow due to a rotating disk. *Frontiers in Heat and Mass Transfer (FHMT).* 2017; **8**

[34] Crane LJ. Flow past a stretching plate. *Zeitschrift für angewandte Mathematik und Physik ZAMP.* 1970; **21**(4):645-647

[35] Sandeep N, Sulochana C, Kumar BR. Unsteady MHD radiative flow and heat transfer of a dusty nanofluid over an exponentially stretching surface. *Engineering Science and Technology, an International Journal.* 2016; **19**(1): 227-240

[36] Nayak MK, Akbar NS, Tripathi D, Khan ZH, Pandey VS. MHD 3D free convective flow of nanofluid over an exponentially stretching sheet with chemical reaction. *Advanced Powder Technology.* 2017; **28**(9):2159-2166

[37] Hayat T, Nadeem S. Flow of 3D Eyring-Powell Fluid by Utilizing Cattaneo-Christov Heat Flux Model and Chemical Processes Over An

Exponentially Stretching Surface. *Results in Physics;* 2017

[38] Rehman FU, Nadeem S, Haq RU. Heat transfer analysis for three-dimensional stagnation-point flow over an exponentially stretching surface. *Chinese Journal of Physics.* 2017; **55**(4): 1552-1560